TISSUE ENGINEERING: Part A
Volume 16, Number 1, 2010

DOI: 10.1089/ten.tea.2009.0074

Biomimetic Modification of Porous TiNbZr Alloy Scaffold for Bone Tissue Engineering

Xiaojian Wang, M.S., Yuncang Li, Ph.D., Peter D. Hodgson, Ph.D., and Cui'e Wen, Ph.D.

Porous titanium (Ti) and Ti alloys are important scaffold materials for bone tissue engineering. In the present study, a new type of porous Ti alloy scaffold with biocompatible alloying elements, that is, niobium (Nb) and zirconium (Zr), was prepared by a space-holder sintering method. This porous TiNbZr scaffold with a porosity of 69% exhibits a mechanical strength of 67 MPa and an elastic modulus of 3.9 GPa, resembling the mechanical properties of cortical bone. To improve the osteoconductivity, a calcium phosphate (Ca/P) coating was applied to the surface of the scaffold using a biomimetic method. The biocompatibility of the porous TiNbZr alloy scaffold before and after the biomimetic modification was assessed using the SaOS2 osteoblast–like cells. Cell culture results indicated that the porous TiNbZr scaffold is more favorable for cell adhesion and proliferation than its solid counterpart. By applying a Ca/P coating, the cell proliferation rate on the Ca/P-coated scaffold was significantly improved. The results suggest that high-strength porous TiNbZr scaffolds with an appropriate osteoconductive coating could be potentially used for bone tissue engineering application.

Introduction

Scaffolds are of great importance for bone tissue engineering and orthopedic implants because they provide good biological fixation to the surrounding tissue through tissue ingrowth into the porous network.[1] Although porous ceramics and polymers have been studied as potential bone graft materials, they cannot meet the mechanical requirements for load-bearing conditions.[2–4] Porous tantalum (Ta) marked under the name of Trabecular Metal™ (Zimmer, Warsaw, IN) has been investigated as pressfit or cementless components for total joint arthroplasty, bone graft substitute, or potential cartilage resurfacing scaffolds.[5–9] These investigations have concluded that porous Ta scaffolds facilitate bone formation[6] and integrate well with both hard[7,8] and soft tissue types.[9] In comparison to Ta, titanium (Ti) is a lightweight and cheaper material and yet has displayed an exceptional biocompatibility in orthopedic and dentistry literature.[10] For this reason, porous Ti and Ti alloys have received increasing research interest. Extensive research has been conducted on fabricating porous Ti using powder or fiber sintering,[11,12] slurry sintering,[13] and rapid prototyping.[13–15] To achieve a porous scaffold possessing both high strength and high porosity simultaneously, porous Ti alloy scaffolds have been developed. A porous Ti-6Al-4V alloy scaffold was reported as achieving greater strength than unalloyed porous Ti at the same porosity.[12,16] However, research on the biological behavior of metals has shown that the composition of implant biomaterials must be carefully selected to avoid or minimize adverse reactions. The release of metal ions from some metal materials, for example, aluminum (Al), nickel (Ni), iron (Fe), vanadium (V), and cobalt (Co), can generate adverse biological effects,[17] but Ti, zirconium (Zr), niobium (Nb), and Ta are believed to be nontoxic metals with good biocompatibility.[10] Therefore, there is a need for research on the development of high-strength porous Ti alloy scaffolds with nontoxic alloying elements for bone tissue engineering.

Metallic implant materials are difficult to bond directly to living bone as a consequence of their limited surface condition. Thus, surface modification by chemical coating process with scaffold materials, such as calcium phosphate (Ca/P), is typically required. The Ca/P synthetic materials are considered osteoconductive biomaterials.[18,19] Ca/P coatings applied on Ti implants have been shown to enhance bone apposition and biological fixation.[20–22] Plasma spraying is the most often-used method for obtaining a Ca/P coating and has achieved commercial success.[23,24] However, plasma spraying is an expensive technique requiring an extremely high operation temperature as 12,000°C. This method also does not allow the accurate control of chemical composition, crystallographic structure, and uniformity of the thickness of the coatings.[25] In comparison to plasma spraying process, biomimetic coating method offers many advantages, for example, better control of the chemical composition of the coating, the possibility to prepare homogeneous film, close structure to bone apatite, a reduction in the densification temperature, and suitable for coating on complex-shaped porous implants.[26] In the present study, Ca/P coatings were

Institute for Technology Research and Innovation, Deakin University, Geelong, Victoria, Australia.

applied on the surface of porous TiNbZr scaffolds by a biomimetic coating method. The structure and mechanical properties of the porous TiNbZr scaffold were studied using scanning electron microscopy (SEM), X-ray diffraction (XRD), and compression tests. The cell attachment and the proliferation of the SaOS2 osteoblast–like cells on the porous scaffolds were investigated.

Materials and Methods

Specimen preparation and characterization

The fabrication method of porous TiNbZr alloy was similar to that used in previous studies.[27–29] Elemental metal powders of Ti (purity >99.7% and particle size <45 μm), Nb (purity >99.8% and particle size <45 μm), and Zr (purity >99.9% and particle size <45 μm) were weighed to give a nominal composition of Ti-10Nb-10Zr (wt.%). The powders were blended in a ball milling system with a ball to powder ratio of 1:2 for 4 h. The blended TiNbZr powder was mixed with ammonium hydrogen carbonate, which was used as the space-holder material. The size selected of the space-holder particles was 500–800 μm in diameter. The mixture of Ti, Nb, Zr powder, and ammonium hydrogen carbonate was cold-pressed into green compacts in a 50-ton hydraulic press, and the green compacts were sintered in two steps. The first step was carried out at 175°C for 2 h to burn out the space-holder particles. In the second step the compacts were heated to 1200°C in a vacuum furnace and held for 10 h in a high vacuum of 10^{-4} to 10^{-5} torr. Porous TiNbZr alloys with a porosity of 69% were fabricated for structure, mechanical properties, Ca/P coating, and biocompatibility tests. To examine the mechanical properties, cylindrical samples with a diameter of 10 mm and a length of 15 mm were used. Porous TiNbZr disc samples with a diameter of 10 mm and a thickness of 2 mm were used for cell culture experiments.

All the samples taken from the furnace were consecutively ground with silicon carbide papers with grits of 240 and 600. The samples were then washed with (i) distilled water, (ii) acetone, (iii) distilled water, and (iv) ethanol in consecutive steps using an ultrasonic bath for 10 min each step. For cell culture, all samples were then sterilized using 70% ethanol for 2 h in an orbital shaker and then air-dried at room temperature in a biohazard hood for 2 h. SEM equipped with an energy-dispersive X-ray spectroscopy (EDX) and XRD were used to characterize the pore structure and phase constituents of the porous alloys. Compression tests were carried out on a 30 kN Instron, equipped with a noncontact extensometer. The initial strain rate was set at 10^{-3} s^{-1}. Significant differences in the compressive strength and elastic modulus were analyzed using one-way analysis of variance ($n = 5$, $p < 0.05$).

Surface modification and Ca/P deposition

The porous TiNbZr samples subjected to alkali treatment were immersed into a 0.5 M NaOH solution (10 mL per sample) and charged in a Teflon-lined autoclave. The autoclave was oven heated at 150°C for 4 h. Porous TiNbZr samples were also treated with 5 M NaOH at 60°C for 24 h for comparison. The porous TiNbZr samples after alkali treatment were washed with diluted HCl (0.05 mM) and distilled water. The porous TiNbZr cylinders after alkali treatment were then heat treated in a vacuum furnace using a heating rate of 5°C per min to 600°C and held for 1 h. Solid pure Ti and TiNbZr alloy discs of the same size, and porous TiNbZr samples without any surface treatment were used as control counterparts.

Ca/P deposition was carried out by soaking the solid and porous Ti and TiNbZr alloy in a simulated body fluid (SBF) for 7 days. A modified 1.5× SBF recipe was used in the present study. The SBF was prepared by dissolving the following chemicals in the sequence of NaCl (8.105 g), $NaHCO_3$ (0.756 g), Na_2CO_3 (0.639 g), KCl (0.338 g), K_2HPO_4 (0.261 g), $MgCl_2 \cdot 6H_2O$ (0.467 g), $CaCl_2$ (0.440 g), and Na_2SO_4 (0.108 g). The solution was buffered to pH 7.40 with HEPES (26.838 g) and 1 M NaOH at 37°C. Each sample was placed in a polyethylene (PE) Petri dish with 30 mL SBF and incubated at 37°C. To keep the ion concentration stable, the SBF solution was refreshed every 2 days. The porous TiNbZr samples after 0.5 M alkali and heat treatment were then soaked in SBF for 1 week.

MTT assay

The cell culture was performed on the solid Ti, TiNbZr alloy sample, and the porous TiNbZr alloy before and after Ca/P coating in 12-well tissue culture plates. SaOS2 osteoblast–like cells (10,000/per well) were seeded on the top surface of the samples. The cells were cultured in the minimum essential medium supplemented with 10% fetal bovine serum, 1% nonessential amino acid, 10,000 units/mL penicillin, 10,000 μg/mL streptomycin, and 0.4% amphostat B at 37°C in a humidified atmosphere of 5% CO_2 and 95% air. The medium was changed every 3 days.

An MTT assay for measuring cell viability and proliferation was used to quantitatively determine the number of viable cells that had attached and grown on the samples. After being cultured for 14 days, an MTT solution was added and incubated with cells for 4 h; cells were then lysed to release and solubilize the purple formazan. Colorimetric analysis and comparison to a standard curve of known viable cell numbers can be used to calculate viable cell numbers for each condition ($n = 3$ for all experimental groups). Significant differences in the cell number were analyzed using one-way analysis of variance ($p < 0.05$). Other samples ($n = 2$) were fixed and then rinsed with phosphate-buffered saline, dehydrated in a graded ethanol series, critical point dried, and examined using SEM.

Results

Structure and morphology of porous TiNbZr scaffold

Figure 1 shows the morphologies of the porous TiNbZr alloys with porosity of 69%. Statistical analysis reveals that the pore size of the porous TiNbZr alloy falls mainly in the range of 300–800 μm. Along with macropores, there are also some micropores present on the cell wall of the porous alloys (Fig. 1b), whose size is in the range of 5–20 μm. Figure 1c and d shows the surface morphologies of the porous TiNbZr after 0.5 M NaOH soaking and heat treatment at 600°C for 1 h. The surface was uniformly covered by a nanofiber layer, with a fiber diameter of 50 nm. Previous studies have shown that this nanofiber layer mainly consists of sodium titanate.[30] The morphology and thickness of the sodium titanate layer can be controlled by adjusting the reaction temperature and NaOH concentration.[30]

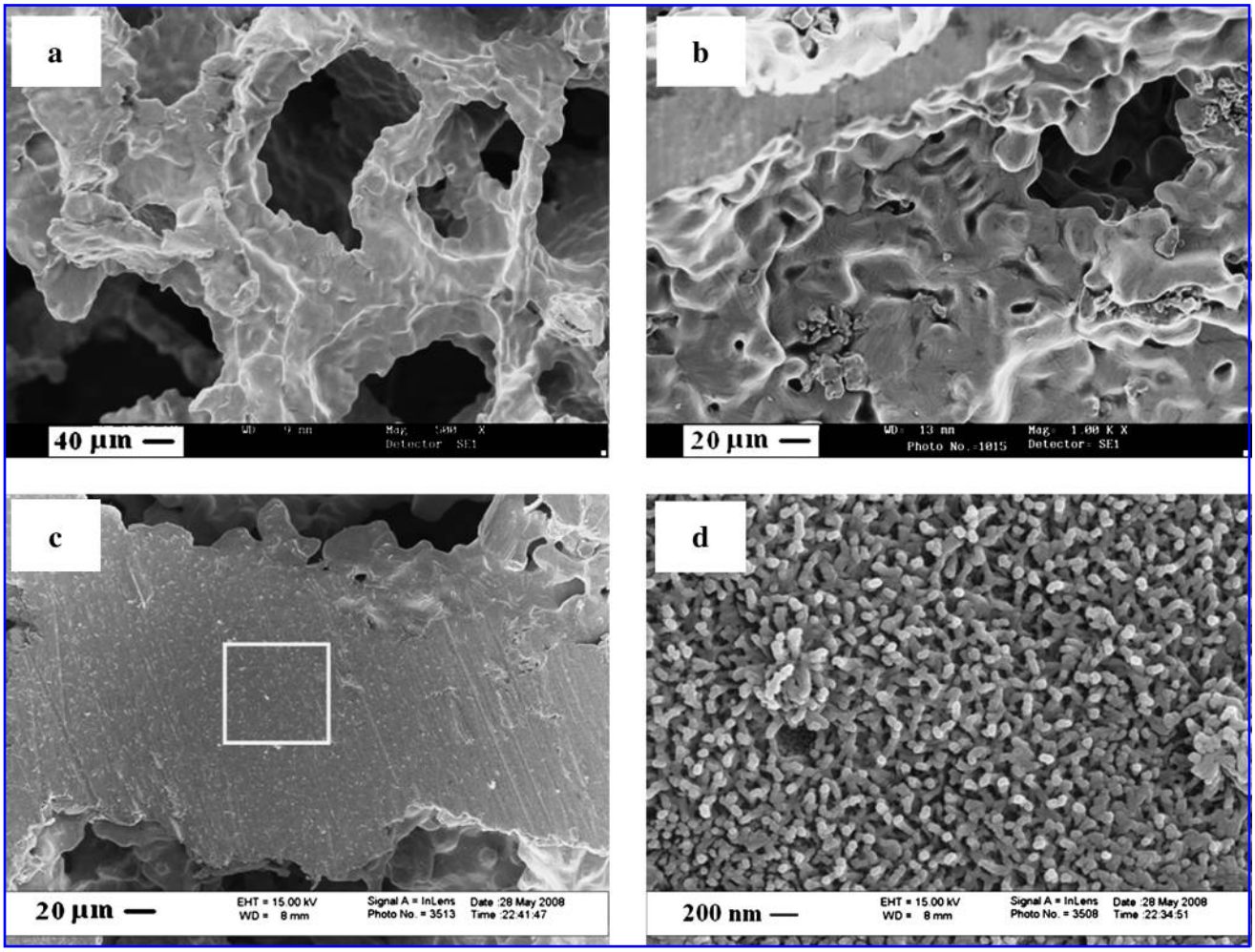

FIG. 1. (**a**) Porous structure of TiNbZr scaffold; (**b**) micropores presenting on the pore walls of the porous TiNbZr; (**c**) surface morphology of the porous TiNbZr scaffold after 0.5 M NaOH and heat treatment; (**d**) enlargement of the box in (**c**) showing the nanostructured surface. Ti, titanium; Nb, niobium; Zr, zirconium.

Mechanical properties of porous TiNbZr before and after surface modification

The mechanical properties of the porous TiNbZr alloys were investigated by compression testing on the cylindrical samples. The compressive stress–strain curves of the porous TiNbZr alloys and surface-treated porous TiNbZr are shown in Figure 2. The stress–strain curves are smooth, implying that the porous alloys exhibit excellent ductility during compression testing. The porous TiNbZr alloy with a porosity of 69% exhibits an elastic modulus and plateau stress of 3.9 GPa and 67 MPa, respectively (Fig. 2, curve a). The compressive strength of porous pure Ti with a porosity of 70% is reported as 53 MPa.[29] The plateau stress of the porous TiNbZr alloy is significantly higher than that of porous pure Ti.

Compressive tests were also carried out on the 0.5 M and 5 M NaOH-treated porous samples, and the stress–strain curves are shown in Figure 2 (curves b and c, respectively). The 5 M NaOH treatment and heat treatment (alkali and heat treatment) were widely used as the method for surface modifying solid Ti and Ti alloys, and this method was shown to be effective in improving the biological performances of Ti-based implant materials, especially bioactivity and bone bonding strength.[31–33] However, the results of the present study show that the alkali treatment caused deterioration to the mechanical strength of the porous alloys. Treatment in 5 M NaOH drastically weakened the strength of the porous alloy. Besides the mechanical strength, the elastic modulus of the porous TiNbZr samples was also decreased after the 5 M NaOH treatment. However, the mechanical strength of 0.5 M NaOH–treated TiNbZr only slightly decreased (Fig. 2, curve b) compared to the untreated samples (Fig. 2, curve a). The alkali and heat treatment is an inherent surface-damaging process. After an alkali treatment, a gel-like layer of sodium titanate covers the surface of Ti, and this gel layer connects to the substrate through a graded oxide layer.[34] The thickness of these two layers may be up to 10 µm, depending on the treatment conditions.[35] As a result, highly corrosive chemical agents are detrimental to the mechanical strength of the surface-modified porous metallic scaffold. Therefore, it can be concluded that although the alkali and heat treatment is an effective method to improve the bioactivity of solid metallic materials, it damages the mechanical properties of a porous metal material. It is recommended that the alkali and heat treatment method for surface modification on porous metallic materials should be prudently selected. The present

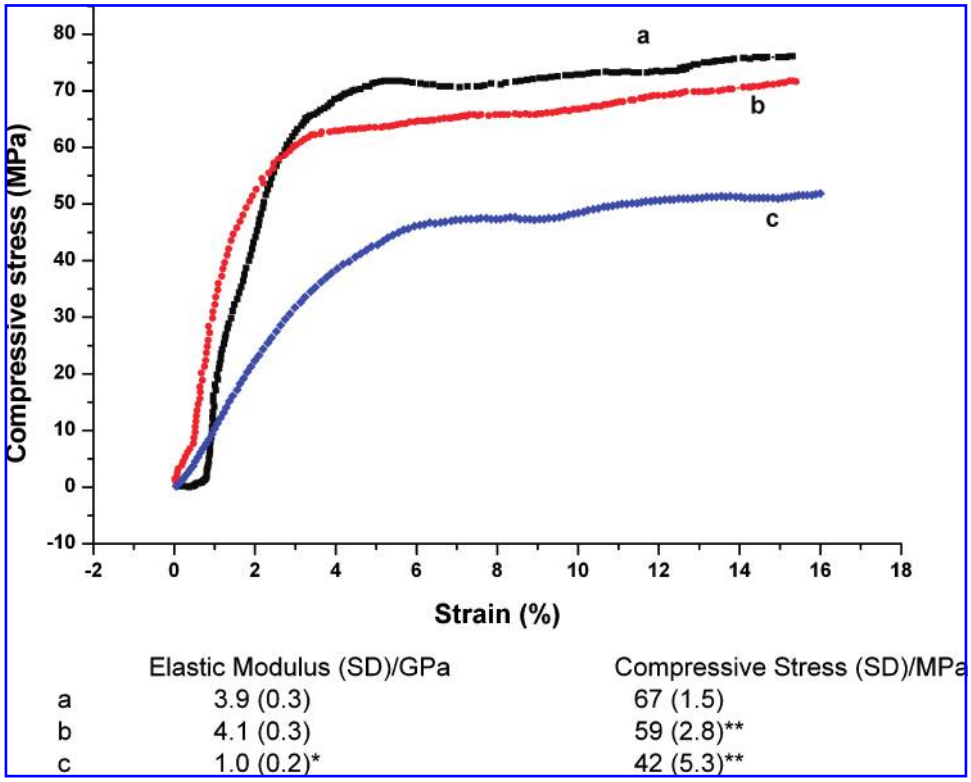

	Elastic Modulus (SD)/GPa	Compressive Stress (SD)/MPa
a	3.9 (0.3)	67 (1.5)
b	4.1 (0.3)	59 (2.8)**
c	1.0 (0.2)*	42 (5.3)**

FIG. 2. Stress-strain curves of porous TiNbZr alloy scaffolds. Untreated porous TiNbZr alloy (curve a), 0.5 M NaOH at 150°C for 4 h and heat treatment at 600°C for 1 h (curve b), and 5 M NaOH at 60°C for 24 h and heat treatment at 600°C for 1 h (curve c). Standard deviations (SD) are shown in parentheses. Significant difference: $^{*}p < 0.05$ and $^{**}p < 0.05$. Color images available online at www.liebertonline.com/ten.

study demonstrated that a relatively low concentration NaOH (i.e., 0.5 M) is suitable for modifying porous Ti alloy scaffold.

Ca/P deposition on porous TiNbZr

Figure 3a shows that a uniform, thin Ca/P layer was deposited on the surface of the 0.5 M alkali and heat–treated porous TiNbZr after it had been soaked in SBF for 1 week. The XRD also confirmed that the layer consisted of hydroxyapatite [$Ca_{10}(PO_4)_6(OH)_2$], as shown in Figure 4. Energy-dispersive X-ray spectroscopy showed that the Ca/P ratio is 1.69. The morphology of Ca/P coating on the porous alloys was similar to that deposited on solid Ti or Ti alloy plates.[36] Small Ca/P nuclei were first deposited on the surface, and then they grew spontaneously by consuming Ca and P ions from the surrounding SBF. These Ca/P particles connected and merged into each other, leading to the formation of a uniform layer. The entire surface came to be covered by the Ca/P layer. Figure 3d reveals that the thickness of this Ca/P layer was about 10 μm. The results show that the porous TiNbZr was homogenously covered with a Ca/P coating after soaking in 1.5× SBF for 1 week.

In vitro *biocompatibility*

SaOS2 osteoblast–like cells showed significant differences in terms of the cell numbers on three types of porous and solid samples after culture for 14 days, as presented in Figure 5. In particular, the cell numbers on the porous scaffolds are shown to be over three times higher than those on solid samples. This is mainly the result of the large surface area of porous material over the solid material. The results indicate that the porous TiNbZr scaffolds are more favorable for cell adhesion and proliferation than the solid counterparts. Cell numbers on all three groups of porous samples were found to be statistically different from one another. The cell numbers were found to yield the highest values on the Ca/P-coated porous scaffold. SEM micrographs, as shown in Figure 6, present the cell morphologies on the porous TiNbZr, surface-treated porous TiNbZr, and Ca/P-coated porous TiNbZr, respectively. There is no significant difference in terms of cell morphology on the three scaffolds. Cells are randomly orientated and polygonally spread on the surfaces of the scaffolds. Cells were observed adhered to the most raised points, suspending themselves by their cytoplasmatic regions over the depressed areas. The MTT results revealed that Ca/P-coated porous TiNbZr favors cell adhesion and proliferation, demonstrated by yielding the highest values of cell numbers after culture for 14 days.

Discussion

The porosity, pore size, and interconnectivity significantly affect the biological performance of porous implant materials.[37] Higher porosity is expected to be beneficial for bone ingrowths. It was reported that dental implants coated with porous Ti with 44% and 48% porosity have been implanted into canine mandibles and femoral.[37] Greater bone ingrowth was found for higher porosity coatings after 14 weeks of implantation. Similarly, bone ingrowth was shown to be deeper and greater in higher porous polymer scaffolds.[38] However, the elastic modulus and compressive strength of a scaffold material decrease with the increase of porosity. For a typical porous material, the relationships between the plateau stress, elastic modulus, and the relative density are given by

$$E/E_s = (\rho/\rho_s) \quad (1)$$

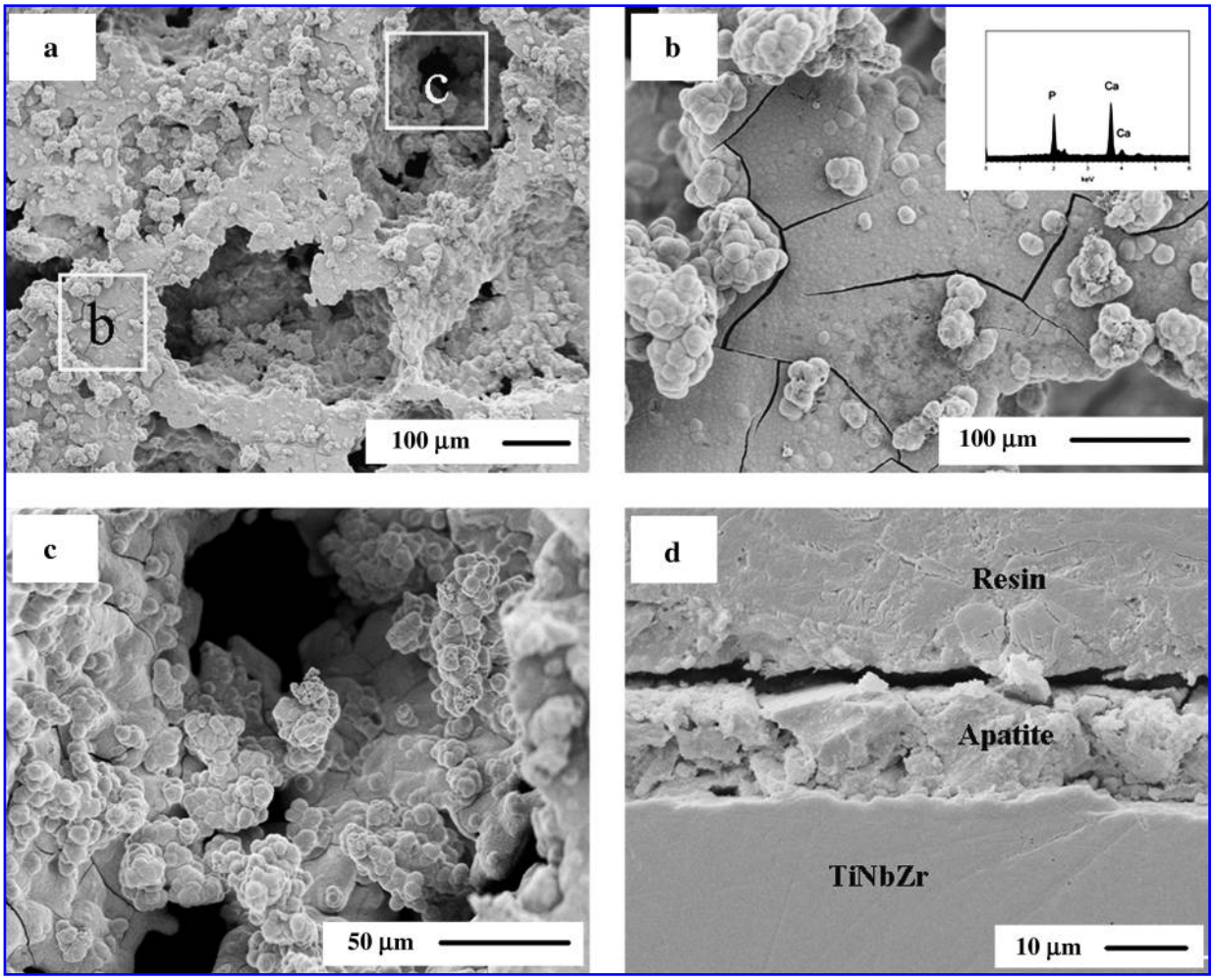

FIG. 3. Ca/P formation on porous TiNbZr scaffolds: (**a**) 0.5 M NaOH–treated porous TiNbZr after soaking in 1.5× simulated body fluid for 1 week; (**b**) Ca/P deposition on the edge of porous TiNbZr scaffold, energy dispersive x-ray spectroscopy (EDX) (inset) shows the coating of Ca/P layer; (**c**) Ca/P deposition inside the pores; (**d**) cross section of Ca/P layer on porous TiNbZr scaffold. Ca/P, calcium phosphate.

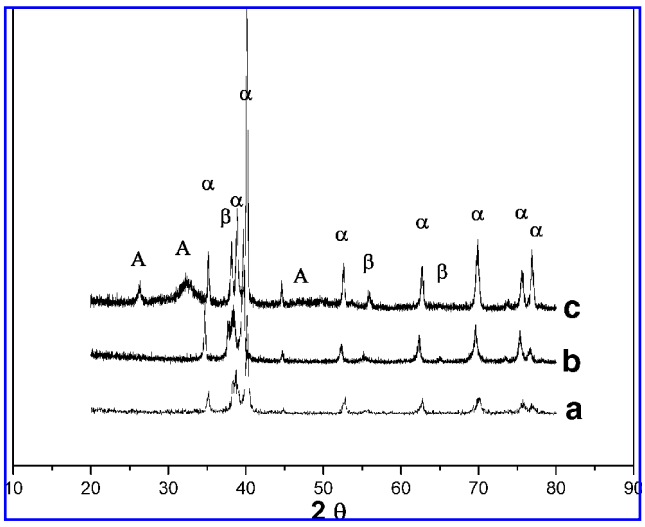

FIG. 4. X-ray diffraction pattern of (**a**) porous TiNbZr after sintering for 10 h; (**b**) porous TiNbZr scaffold after 0.5 M NaOH soaking and heat treatment; (**c**) porous TiNbZr scaffold after 0.5 M alkali and heat treatment and 1.5× simulated body fluid soaking for 1 week. α, alpha phase titanium; β, beta phase titanium; A, apatite.

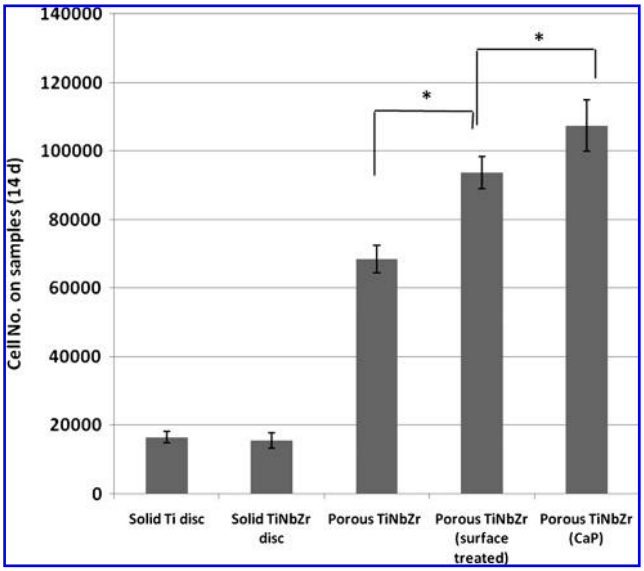

FIG. 5. MTT results of solid Ti, solid TiNbZr discs, and porous TiNbZr scaffolds, after culture for 14 days. Significant difference: $^{*}p < 0.05$.

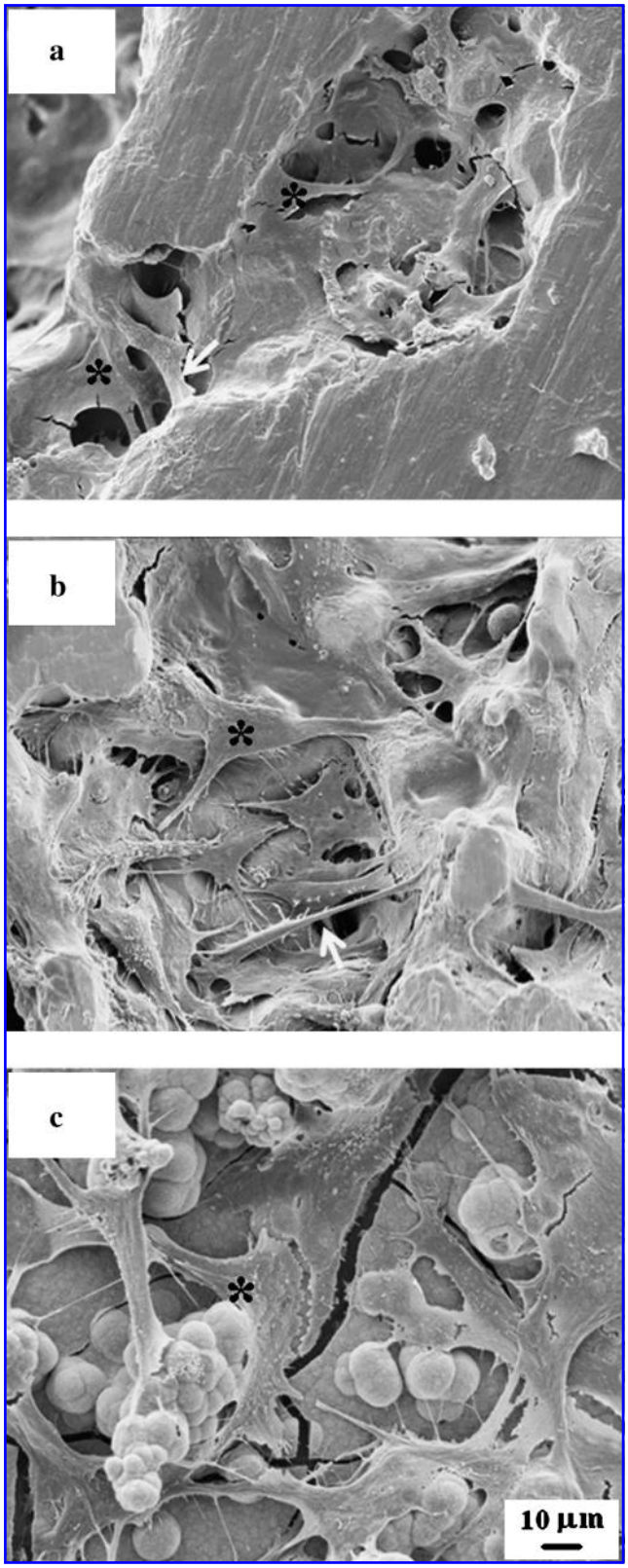

FIG. 6. Cell adhesion and proliferation on (**a**) porous TiNbZr, (**b**) porous TiNbZr after 0.5 M NaOH and heat treatment, and (**c**) Ca/P-coated porous TiNbZr. Arrows and asterisks indicate cells' spreading on the scaffolds.

$$\sigma_{pl}/\sigma_{ys} = 0.3(\rho/\rho_s)^{3/2} \quad (2)$$

where E is the elastic modulus of the foam, E_s is the elastic modulus of the cell edge solid materials, σ_{pl} is the plateau stress of the porous material, and σ_{ys} is the yield strength of the cell edge solid material.[39] Therefore, a porous material could combine sufficient mechanical strength and high porosity at the same time only if the cell edge solid material possesses high yield strength. The present study demonstrated that the porous TiNbZr scaffold with a porosity of 69% exhibits a mechanical strength of 67 MPa and an elastic modulus of 3.9 GPa. The mechanical strength of the TiNbZr scaffolds is significantly higher than that of pure Ti scaffolds (53 MPa[29]), at the same porosity. It was reported that porous Ta with a porosity of 65–73% had a yield strength of 35.2 MPa and an elastic modulus of 1.15 GPa.[40] The porous TiNbZr exhibits higher mechanical strength than the porous Ta at the same porosity level.

Synthetic Ca/P materials are considered to be osteoconductive biomaterials.[18,19] The Ca/P coating on an implant surface significantly enhances the initial fixation and ultimate osseous integration. Comparative studies have indicated implants of similar design, with Ca/P-coated femoral stems achieving more reliable bony fixation than their porous control groups.[18] The Ca/P coating enhanced human bone marrow–derived mesenchymal cell phenotypic osteogenic lineage (osteopontin and osteonectin) and osteoblast synthetic activity (alkaline phosphatase activity, collagen type I, and osteoprotegerin).[41] On the other hand, the bulk composition of implants also has an effect on osteointegration process. *In vitro* test showed that osteoblast synthetic activities were enhanced when cultured on Ca/P-coated Ti13Nb13Zr plates, compared to Ca/P-coated Ti6Al4V plates.[42] Further, higher bone maturation was observed on Ca/P-coated Ti13Nb11Zr implant.[42] The results indicated that both alloy composition and HA coating affect bone response around metallic implants. In the present work, Ca/P-coated porous TiNbZr scaffolds were shown to favor SaOS2 osteoblast–like cell adhesion and proliferation. Cells were randomly orientated and were polygonally spread on the surfaces of the scaffolds. By applying a Ca/P coating, more cells attached and proliferated throughout of the porous TiNbZr scaffold, compared with the uncoated samples. Scaffold materials implanted in the bone will encounter complicated conditions compared to *in vitro* conditions, such as more and different cell types and local strain.[13] Porous Ti scaffolds from this group have been investigated for healing of bone defects in a canine model.[43] The porous Ti scaffolds exhibited good biocompatibility, and allowed for bone ingrowth throughout the interconnected pores. Consequently, further *in vivo* studies will be carried out on porous TiNbZr alloy with and without Ca/P coating to understand how bone interacts with the scaffolds.

Conclusions

Open-cell porous TiNbZr alloy scaffolds with a porosity of 69% were prepared by a space-holder sintering method. The porous TiNbZr exhibits a high mechanical strength of 67 MPa and an elastic modulus of 3.9 GPa, resembling the mechanical properties of cortical bone, with a porous structure similar to that of trabecular bone. The porous TiNbZr

scaffold surface treated with 0.5 M NaOH at 150°C exhibits a nanostructured surface that can effectively induce Ca/P nucleation when soaking in SBF. A Ca/P layer, with a thickness of 10 μm, uniformly covered the surface-treated porous TiNbZr after soaking in 1.5× SBF for 1 week. Cell culture experiments showed that the porous TiNbZr scaffold is more favorable for the SaOS2 osteoblast-like cell adhesion and proliferation than its solid counterpart. By applying a Ca/P coating, more cells attached and proliferated throughout of the porous TiNbZr scaffold.

Acknowledgments

The authors acknowledge the financial support for this research through the Australian Research Council (ARC) Discovery Project DP0770021. P.D.H. was also supported by the ARC through a Federation Fellowship.

Disclosure Statement

No competing financial interests exist.

References

1. Kujala, S., Ryhanen, J., Danilov, A., and Tuukkanen, J. Effect of porosity on the osteointegration and bone ingrowth of a weight-bearing nickel-titanium bone graft substitute. Biomaterials **24,** 4691, 2003.
2. Hing, K.A., Best, S.M., Tanner, K.E., Bonfield, W., and Revell, P.A. Mediation of bone ingrowth in porous hydroxyapatite bone graft substitutes. J Biomed Mater Res **68A,** 187, 2004.
3. de Long, W.G., Einhorn, T.A., Koval, K., McKee, M., Smith, W., Sanders, R., and Wstson, T. Bone grafts and bone graft substitutes in orthopaedic trauma surgery. A critical analysis. J Bone Joint Surg **89,** 649, 2007.
4. Yoshikawa, H., and Myoui, A. Bone tissue engineering with porous hydroxyapatite ceramics. J Artif Organs **8,** 131, 2005.
5. Levine, B.R., Sporer, S., Poggie, R.A., Della Valle, C.J., and Jacbs, J.J. Experimental and clinical performance of porous tantalum. Biomaterials **27,** 4671, 2006.
6. Zou, X., Li, H., Bunger, M., Egund, N., Lind, M., and Bunger, C. Bone ingrowth characteristics of porous tantalum and carbon fiber interbody devices: an experimental study in pigs. Spine J **4,** 99, 2004.
7. Bobyn, J.D., Glassman, A.H., Goto, H., Krygier, J.J., Miller, J.E., and Brooks, C.E. The effect of stem stiffness on femoral bone resorption after canine porous-coated total hip arthroplasty. Clin Orthop Relat Res **261,** 196, 1990.
8. Bobyn, J.D., Stackpool, G.J., Hacking, S.A., Tanzer, M., and Krygier, J.J. Characteristics of bone ingrowth and interface mechanics of a new porous tantalum biomaterial. J Bone Joint Surg Br **81,** 907, 1999.
9. Hacking, S.A., Bobyn, J.D., Toh, K., Tanzer, M., and Krygier, J.J. Fibrous tissue ingrowth and attachment to porous tantalum. J Biomed Mater Res **52,** 631, 2000.
10. Long, M., and Rack, H.J. Titanium alloys in total joint replacement—a materials science perspective. Biomaterials **19,** 1621, 1998.
11. Oh, I.H., Nomura, N., Masahashi, N., and Hanada, S. Mechanical properties of porous titanium compacts prepared by powder sintering. Scr Mater **49,** 1197, 2003.
12. Li, J.P., de Wijn, J.R., van Blitterswijk, C.A., and de Groot, K. Porous Ti6Al4V scaffold directly fabricating by rapid prototyping: preparation and *in vitro* experiment. Biomaterials **27,** 1223, 2006.
13. Li, J.P., Li, S.H., van Blitterswijk, C.A., and de Groot, K. A novel porous Ti6Al4V: characterization and cell attachment. J Biomed Mater Res **73A,** 223, 2005.
14. Hollander, D.A., von Walter, M., Wirtz, T., Sellei, R., Schmidt-Rohlfing, B., Paar, O., and Erli, H.-J. Structural, mechanical and *in vitro* characterization of individually structured Ti-6Al-4V produced by direct laser forming. Biomaterials **27,** 955, 2006.
15. Ryan, G.E., Pandit, A., and Apatsidis, D.P. Porous titanium scaffolds fabricated using a rapid prototyping and powder metallurgy technique. Biomaterials **29,** 3625, 2008.
16. Heinl, P., Müller, L., Körner, C., Singer, R.F., and Müller, F.A. Cellular Ti-6Al-4V structures with interconnected macro porosity for bone implants fabricated by selective electron beam melting. Acta Biomater **4,** 1536, 2008.
17. Okazaki, Y., Rao, S., Tateishi, T., and Ito, Y. Cytocompatibility of various metal and development of new titanium alloys for medical implants. Mater Sci Eng A **243,** 250, 1998.
18. Dalton, J.E., Cook, S.D., Thomas, K.A., and Kay, J.F. The effect of operative fit and hydroxyapatite coating on the mechanical and biological response to porous implants. J Bone Joint Surg Am **77,** 97, 1995.
19. Froimson, M.I., Garino, J., Machenaud, A., and Vidalain, J.P. Minimum 10-year results of a tapered, titanium, hydroxyapatite-coated Hip stem. J Arthroplasty **22,** 1, 2007.
20. Daculsi, G. Biphasic calcium phosphate concept applied to artificial bone, implant coating and injectable bone substitute. Biomaterials **19,** 1473, 1998.
21. Zhang, Q., Leng, Y., and Xin, R. A comparative study of electrochemical deposition and biomimetic deposition of calcium phosphate on porous titanium. Biomaterials **26,** 2857, 2005.
22. Habibovic, P., Li, J., van der Valk, C.M., Meijer, G., Layrolle, P., van Blitterswijk, C.A., and de Groot, K. Biological performance of uncoated and octacalcium phosphate-coated Ti6Al4V. Biomaterials **26,** 23, 2005.
23. Berndt, C.C., Haddad, G.N., Farmer, A.J.D., and Gross, K.A. Spraying for bioceramic applications-A review. Mater Forum **14,** 161, 1990.
24. Frayssinet, P., Hardy, D., Rouquet, N., Giammara, B., Guilhem, A., and Hanker, J. New observations on middle term hydroxyapatite-coated titanium alloy hip prosthesis. Biomaterials **13,** 668, 1992.
25. Lavos-Valereto, I., Deboni, M., and Azambuja, N. Evaluation of the titanium Ti-6Al-7Nb alloy with and without plasma-sprayed hydroxyapatite coating on growth and viability of cultured osteoblast-like cells. J Periodontol **73,** 900, 2002.
26. Kokubo, T., Miyaji, F., and Kim, H.M. Spontaneous formation of bonelike apatite layer on chemically treated titanium metals. J Am Ceram Soc **79,** 1127, 1996.
27. Wang, X.J., Li, Y., Xiong, J.Y., Hodgson, P.D., and Wen, C.E. Porous TiNbZr alloy scaffolds for biomedical applications. Acta Biomater. DOI:10.1016/j.actbio.2009.06.002, 2009. (In press)
28. Wen, C.E., Mabuchi, M., Yamada, Y., Shimojima, K., Chino, Y., and Asahina, T. Processing of biocompatible porous Ti and Mg. Scr Mater **45,** 1147, 2001.
29. Wen, C.E., Yamada, Y., Shimojima, K., Sakaguchi, Y., Chino, Y., Hosokawa, H., and Mabuchi, M. Novel titanium foam for bone tissue engineering. J Mater Res **17,** 2633, 2002.
30. Wang, X.J., Li, Y.C., Lin, J.G., Yamada, Y., Hodgson, P.D., and Wen, C.E. *In vitro* bioactivity evaluation of titanium and niobium metals with different surface morphologies. Acta Biomater **4,** 1530, 2008.

31. Fujibayashi, S., Neo, M., Kim, H.Y., Kokubo, T., and Nakamura, T. Osteoinduction of porous bioactive titanium metal. Biomaterials **25,** 443, 2005.
32. Kokubo, T., and Takadama, H. How useful is SBF in predicting *in vivo* bone bioactivity? Biomaterials **27,** 2907, 2006.
33. Nishiguchi, S., Kato, H., Fujita, H., Oka, M., Kim, H.M., Kokubo, T., and Nakamura, T. Titanium metals form direct bonding to bone after alkali and heat treatments. Biomaterials **22,** 2525, 2001.
34. Kim, H.M., Himeno, T., Kawashita, M., Lee, J.H., Kokubo, T., and Nakamura, T. Surface potential change in bioactive titanium metal during the process of apatite formation in simulated body fluid. J Biomed Mater Res **67A,** 1305, 2003.
35. Dong, W., Zhang, T., Epstein, J., Cooney, L., Wang, H., Li, Y., Jiang, Y.B., Cogbill, A., Varadan, V., and Tian, Z.R. Multifunctional nanowire bioscaffolds on titanium. Chem Mater **19,** 4454, 2007.
36. Wang, X.J., Li, Y.C., Lin, J.G., Hodgson, P.D., and Wen, C.E. Apatite-inducing ability of titanium oxide layer on titanium surface: the effect of surface energy. J Mater Res **23,** 1682, 2008.
37. Story, B.J., Wagner, W.R., Gaisser, D.M., Cook, S.D., and Rust-Dawicki, A.M. *In vivo* performance of a modified CSTi dental implant coating. Int J Oral Maxillofac Surg **13,** 749, 1998.
38. Lewandrowski, K.U., Gresser, J.D., Bondre, S., Silva, A.E., Wise, D.L., and Trantolo, D.J. Developing porosity of poly (propyleneglycol-co-fumaric acid) bone graft substitutes and the effect on osteointegration: a preliminary histology study in rats. J Biomater Sci Polym Ed **11,** 879, 2000.
39. Gibson, L.G., and Ashby, M.F. Cellular Solids: Structure and Properties, second edition. Cambridge: Cambridge University Press, 1997.
40. Sevilla, P., Aparicio, C., Planell, J.A., and Gil, F.J. Comparison of the mechanical properties between tantalum and nickel-titanium foams implant materials for bone ingrowth applications. J Alloy Compd **439,** 67, 2007.
41. Bigi, A., Nicoli-Aldini, N., Bracci, B., Zavan, B., Boanini, E., Sbaiz, F., Panzavolta, S., Zorzato, G., Giardino, R., Facchini, A., Abatangelo, G., and Cortivo, R. *In vitro* culture of mesenchymal cells onto nanocrystalline hydroxyapatite-coated Ti13Nb13Zr alloy. J Biomed Mater Res **82A,** 213, 2007.
42. Bigi, A., Fini, M., Bracci, B., Boanini, E., Torricelli, P., Giavaresi, G., Aldini, N.N., Facchini, A., Sbaiz, F., and Giardino, R. The response of bone to nanocrystalline hydroxyapatite-coated Ti13Nb11Zr alloy in an animal model. Biomaterials **29,** 1730, 2008.
43. Faria, P.E.P., Carvalho, A.L., Felipucci, D.N.B.F., Wen, C.E., Sennerby, L., and Salata, L.A. Bone formation following implantation of titanium sponge rods into humeral osteotomies in dogs: a histological and histometrical study. Clin Implant Dent Relat Res. DOI: 10.1111/j.1708 8208.2008. 00132.x, 2009. (In press)

Address correspondence to:
Cui'e Wen, Ph.D.
Institute for Technology Research and Innovation
Deakin University
Geelong
Victoria 3217
Australia

E-mail: cwen@deakin.edu.au

Received: February 3, 2009
Accepted: August 24, 2009
Online Publication Date: September 28, 2009